

- 29 -

## **SIMULATION OF ELECTRICAL POTENTIAL DIFFERENCES NEAR A CONTAMINANT PLUME EXCITED BY A POINT SOURCE OF CURRENT**

by  
James L. Osiensky<sup>1</sup>, Roy E. Williams<sup>1</sup>, Dale R. Ralston<sup>1</sup>,  
Gary S. Johnson<sup>1</sup> and Leland L. Mink<sup>2</sup>

### **ABSTRACT**

Finite-difference simulations of electrical excitation of conductive contaminant plumes indicated that the approximate dimensions of a plume and the approximate location of its center of mass can be derived, under specified circumstances, from the resulting electrical potential fields. Direct electrical excitation of a contaminant plume by a point current source was simulated for homogenous and isotropic conditions as well as in the presence of conductive clay layers and lenses. When a very shallow water table was assumed, changes in the electrical potential field between baseline (preplume) conditions and conditions that included a developing plume graphically formed a difference dipole. Simulations suggested that electrical flow is channeled preferentially through the negative difference pole at the approximate location of the center of mass in a dispersive contaminant plume. Electrical flow was channeled directly through the negative difference pole at the terminal end of a conductive clay lens. Simulations showed that even in the presence of conductive clays, the approximate location of the center of mass of an evolving contaminant plume could be delineated. This illustrates the potential future value of this approach, assuming continued technological advances in the field.

### **INTRODUCTION**

Ground water monitoring programs generally are designed to show that contamination does not exist, is contained within specific boundaries, or will be detected immediately if it occurs. The literature is replete with case histories that used surface electrical resistivity methods to help detect contaminated ground water.

A single current electrode method known as the *mise-a-la-masse* method was first described by Schlumberger (1920). To date, most published applications of the *mise-a-la-masse* method involve mining applications that provided qualitative information on the extent and continuity of metallic ore bodies. With this method, an electrical current is passed directly into an ore body while steady state electrical potentials are measured at the land surface or in boreholes (Parasnis, 1967). Ketola (1972) described measurements made to map ore bodies in Finland. Mansinha and Mwenifumbo (1983) delineated two vein-type mineralized zones in Canada. Eloranta (1985) compared measurements obtained with different electrode arrangements. Eloranta (1986)

---

<sup>1</sup> Hydrology Program, Department of Geology and Geological Engineering, University of Idaho, Moscow, Idaho 83844-3022;

<sup>2</sup> Director, Idaho Water Resources Research Institute, University of Idaho, Moscow, Idaho 83844-3011

described the electrical potential field from a single current electrode near a vertical contact. Bowker (1987) described electrical potential field measurements to evaluate the size of slab-like ore bodies. Dey and Morrison (1979) simulated the three-dimensional potential distribution from an electrical point source for an arbitrary three-dimensional distribution of conductivity. Newkirk (1982) used a three-dimensional model to interpret apparent resistivity responses for three-dimensional bodies near a buried electrode. Beasley and Ward (1986) used a three-dimensional model to simulate the electrical potential field from a single current electrode near fracture zones. They modeled thin conductive bodies with orientations of vertical, horizontal, 30 degrees, and 60 degrees. Beasley and Ward (1986) found that the maximum depth at which a body can be detected at the land surface depends on the position of the current electrode and the contrast in conductivity. Wilt and Tsang (1985) used the 3-dimensional model of Dey and Morrison (1979) to simulate changes in apparent resistivity due to the presence of a buried prism of contaminated ground water within an aquifer. They concluded that the *mise-a-la-masse* method may be used to roughly characterize the contaminant mass and its boundaries. Bevc and Morrison (1989; 1991) showed that a strong asymmetric anomaly (difference dipole as referred to later) developed during a salt water injection experiment when baseline electrical potential data were subtracted from post-injection data. Osiensky and Donaldson (1994; 1995) and Osiensky (1995) showed that the *mise-a-la-masse* method can be useful for the delineation of tracer plumes. However, the degree of success depends on the conductivity contrast between the plume and its surroundings.

The *mise-a-la-masse* method allows the direct measurement of the electrical potential field for existing (often unidentified) boundary conditions. The resulting electrical potential field incorporates all factors that contribute to its development at the particular time of measurement. Subsequent changes that occur over time can be evaluated where the baseline electrical potential field can be measured. The effects of an evolving contaminant plume can be delineated if subsequent data sets are collected under the same conditions as baseline data (e.g., similar moisture content and temperature of surface soils, same depth to the water table, etc.).

### MODEL DEVELOPMENT

Jansen and Taylor (1995) showed that the ground water flow code MODFLOW (McDonald and Harbaugh, 1988) could be used to simulate electrical geophysical methods. Osiensky and Williams (1996) and Osiensky (1997) presented mathematical justification for use of the MODFLOW (McDonald and Harbaugh, 1988) code to simulate electrical flow through conductive contaminant plumes. Osiensky (1997) showed by the simulation of electrical flow through six different plumes that the center of mass of an evolving, conductive plume can be tracked by measurement of the resulting electrical potential fields over time.

In this paper, seven different hypothetical, hydrogeological scenarios were simulated using a much finer horizontal and vertical discretization scheme than those used by Osiensky and Williams (1996) and Osiensky (1997). The test scenarios simulated the presence of a 3-dimensional, conductive contaminant plume in a homogeneous, isotropic aquifer as well as in the presence of layers and lenses of conductive clay. However, they are necessarily limited by the assumptions made and should not be generalized to other potential situations without additional work. For example, no attempt was made in this study to evaluate the maximum depth at which

the plumes could be delineated or to simulate the geometries of all possible geological conditions.

The electrical conductivity -- hydraulic conductivity relationship for each simulation was:

$$\sigma_m = K \quad \text{Eq.1}$$

where:  $\sigma_m$  is the electrical conductivity and  $K$  is the hydraulic conductivity of the porous medium.

Consistent units were used in each simulation (Osiensky and Williams,1996; Osiensky,1997):

- 1) One meter of hydraulic head equaled 1 volt of electrical potential;
- 2) A well injection rate of 0.5 m<sup>3</sup>/d equaled a current injection rate of 0.5 amperes; and an aquifer hydraulic conductivity of 0.01 m/d equaled a baseline electrical conductivity of 0.01 S/m.

#### General Baseline Conditions

General baseline conditions for the simulations consisted of a homogeneous and isotropic block of aquifer material. The block had the dimensions 210 m X 210 m X 1000 m (x, y, z). The homogeneous and isotropic material had an  $\sigma_m = 0.01$  S/m. Each electrical simulation consisted of a 210 x 210 grid with 1 m uniform grid spacing ( $\Delta x, \Delta y$ ) and 33 layers. Layers 1 through 18 were each 1 m thick. Each succeeding layer (layers 19 through 33) increased in thickness by a factor of about 1.5 times the thickness of the adjacent overlying layer.

An injection well with 1 m of well screen was located in layer 1 near the center of the grid (*i.e.*, node (106,105)) to approximate the conditions of a single point, current electrode (metal stake). Calculated (theoretical) constant, electrical potential boundaries were placed along the perimeter of the grid in each layer based on  $\sigma_m = 0.01$  S/m and the individual cell distances from the surface point electrode according to:

$$V = \left( \frac{I}{2\pi\sigma_m} \right) \frac{1}{r} \quad \text{Eq.2}$$

where:  $V$  is the electrical potential (voltage),  $I$  is the total current, and  $r$  is distance.

Electrical potential boundaries were identical for all simulations. Variations in  $\sigma_m$ , due to the presence of clay layers or lenses, were superimposed onto the homogeneous and isotropic material properties at specific, defined locations for each simulation. All simulated clay layers and lenses had  $\sigma_m = 0.25$  S/m. Therefore, each of the seven simulations represented different hydrogeological baseline conditions, except for the boundary conditions.

Plume Development

Concentration data for the hypothetical, 3-dimensional contaminant (non-reactive) plume were developed by the Extended Pulse Approximation method for continuous finite source problems (Domenico and Robbins, 1985; McClymont and Schwartz, 1987). The plume emanated from a shallow, 1 m<sup>2</sup> continuous source with a concentration of 20,000 mg/l for a period of 1.7 years. The advection rate was 3.3 X 10<sup>-7</sup> m/s. Aquifer dispersivity values were 3 m in the x direction, 0.08 m in the y direction and 0.03 m in the z direction. Three-dimensional plume concentrations were generated by the Extended Pulse Approximation on 1 m spacings (Δx, Δy, Δz), based on the work of Domenico and Robbins (1985):

$$C(x,y,z,t) = \left( C_o / 8 \right) \text{erfc} \left[ \frac{(x-vt)}{2(D_x t)^{1/2}} \right] \left\{ \text{erf} \left[ \frac{(y+Y/2)}{2(D_y x/v)^{1/2}} \right] - \text{erf} \left[ \frac{(y-Y/2)}{2(D_y x/v)^{1/2}} \right] \right\} \left\{ \text{erf} \left[ \frac{(z+Z/2)}{2(D_z x/v)^{1/2}} \right] - \text{erf} \left[ \frac{(z-Z/2)}{2(D_z x/v)^{1/2}} \right] \right\} \quad \text{Eq.3}$$

Source and plume concentrations (TDS) in mg/l were converted to ground water electrical conductivity (σ<sub>w</sub>) values in S/m by assuming σ<sub>w</sub> = TDS/6500 (Freeze and Cherry, 1979).

Baseline and plume ground water σ<sub>w</sub> values were converted directly to σ<sub>m</sub> values for each finite-difference cell in MODFLOW by the Archie (1942) formula, as was done by Keller (1987):

$$\sigma_m = a \sigma_w S^n \phi^m \quad \text{Eq.4}$$

where: σ<sub>m</sub> is the electrical conductivity of the porous medium [S/m], φ is the porosity (assumed here to be 0.30), S is the fraction of pores containing water (i.e., S=1 for complete saturation), σ<sub>w</sub> is the electrical conductivity of the pore water [S/m], n is usually close to 2.0 if more than 30% of the pore space is filled with water (Parasnis, 1997), a and m are empirical constants used to force the formula to fit the behavior of the rock type of interest (Keller, 1987). Values for m range between 1.3 in loosely packed granular media to about 2.2 in well-cemented granular rocks (Parkhomenko, 1967). The values for a and m used were 0.88 and 1.37, respectively.

For the conditions used in the Archie formula, baseline σ<sub>w</sub> = 0.0591 S/m was equal to a total dissolved solids concentration of 384 mg/l. These values yielded a baseline σ<sub>m</sub> = 0.01 S/m. By comparison, the plume source concentration of 20,000 mg/l yielded a σ<sub>m</sub> = 0.53 S/m.

Baseline and plume σ<sub>m</sub> values represent the hydraulic conductivity values used as input for each cell of the MODFLOW model (i.e., σ<sub>m</sub> = K). The plume conditions were superimposed (numerically added to the baseline) such that each plume extended northward from the contaminant source located at the cell corresponding to the injection node (106,105). Maximum dimensions of the plume were 50 m long by 15 m wide by 6 m thick discretized into 1 m<sup>3</sup> cells

- 33 -

for the purpose of the simulations. Predicted plume concentrations less than 1 mg/l ( $\sigma_w=0.00015$  S/m) were truncated to keep the size of the plume manageable for the electrical simulations. Figure 1 shows longitudinal electrical conductivity profiles along the centerline of the six layer plume. Note that the center of mass  $\left[ \frac{C}{C_0} = 0.5 \right]$  was located 3 m north of the plume source (current injection point). Identical plume conditions (for comparison purposes) were superimposed onto different, baseline, hydrogeological conditions in each simulation. Each of the following simulations represented shallow plume conditions. However, Beasley and Ward (1986) showed that depth to the conductive body does not significantly affect the pattern of the electrical potentials measured. However, depth to the conductive body does affect the magnitude of the electrical potentials. Therefore, depth to the conductive body usually is the major factor that controls whether electrical methods will be successful with the currently available instrumentation. It should be noted that advances in technology will, with time, increase sensitivity and signal selectivity; the simulations reported on in this paper, though not currently practical, are intended to show the potential future value of this approach.

#### Simulation 1

Baseline conditions for simulation 1 consisted of a homogeneous and isotropic aquifer with an electrical conductivity  $\sigma_m=0.01$  S/m. A steady electric current of 0.5 amperes was injected into node (106,105) for this and all subsequent simulations. Figure 2 shows the baseline (primary), electrical potential field ( $E_0$ ) measured in layer 1 of the model. Figure 3 shows the new (secondary), electrical potential field ( $E_s$ ) measured in layer 1 when the electric current was injected directly into the southernmost tip (*i.e.*, source) of the conductive plume. The distorted electrical potential field shows that electrical equipotential lines tended to deflect due to the presence of the plume. Based on Figure 3 alone, without baseline data, it would not be possible to differentiate between the effects of the plume and the effects of a conductive medium such as a clay layer or lens.

Figure 4 is a contour map of the numerical differences (negative and positive) (referred to as the difference dipole) between  $E_0$  (figure 2) and  $E_s$  (figure 3). Figure 4 graphically represents changes in the distribution of electrical potentials between measurements taken 1.7 years apart. During the 1.7 year period between measurements, the plume can be assumed to have evolved into place. Changes in the distribution of electrical potentials were due solely to the presence of the new dispersive plume extending from the point of current injection. The most significant features of the difference dipole shown in figure 4 were: 1) the positive difference pole at the point of current injection; 2) the negative difference pole near the center of mass (*i.e.*,  $\frac{C}{C_0} = 0.5$ )

of the plume; and 3) the vector extending from the positive difference pole to the negative difference pole positioned along the centerline of the plume and pointed in the direction of plume migration. In addition, the length of the vector approximated the distance that the center of mass migrated over time. Note: difference dipoles are presented in absolute terms (millivolts), rather than as a percentage relative to the baseline data set. Small differences shown in some cases may not be measurable under actual field conditions with currently available instrumentation.

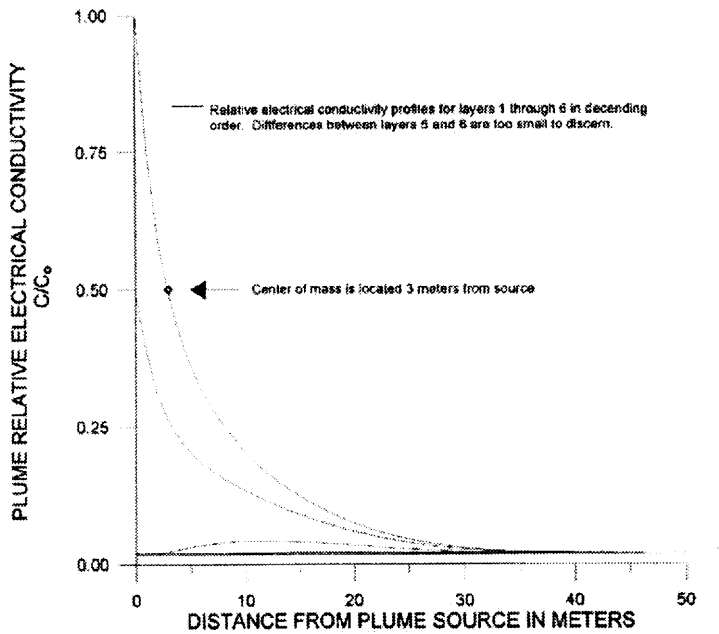


Figure 1. Electrical conductivity distribution along the centerline of the plume.

### Simulation 2

Baseline conditions for simulation 2 were the same as for simulation 1 (Figure 2). In this simulation, a clay body with the identical shape and extent as the contaminant plume in simulation 1 but with uniform  $\sigma_m = 0.25$  S/m was superimposed onto baseline conditions.

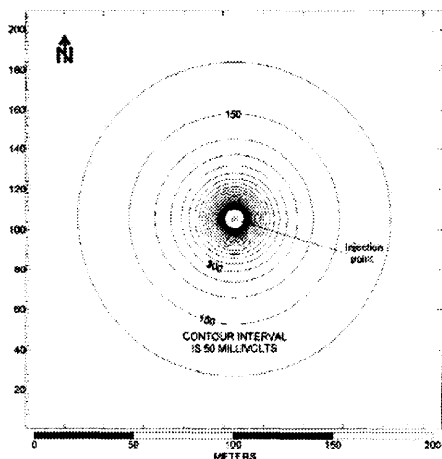


Figure 2. Difference dipole between the baseline electrical potential field with a buried transverse-trending clay lens and the electrical potential field with a plume located above the lens.

While this simulation was unrealistic from the standpoint that a clay body would not develop between measurement periods, it provided a useful basis for comparison. Figure 5 shows the  $E_s$  that would be measured in layer 1 if the electric current is injected directly into the southernmost tip of the clay body. The resulting field is typical of what would be expected in a mise-a-lamasse survey of an ore body of uniform electrical conductivity (Parasnis, 1997). The equipotential lines tended to bend around the clay body forming an approximate outline of its extent and trend. This  $E_s$  clearly was different from the one formed by the dispersive, contaminant plume with a nonuniform electrical conductivity distribution (figure 3). Figure 6 is a contour map of the difference dipole between  $E_0$  (figure 2) and  $E_s$  (figure 5). Of particular interest is the location of the negative difference pole at the northernmost end of the uniformly conductive body. Electrical flow was channeled preferentially to the end of the body compared to the center of mass for the dispersive plume.

### Simulation 3

Baseline conditions for simulation 3 consisted of an aquifer underlain by a conductive ( $\sigma_m = 0.25$  S/m) clay layer. The clay layer extended over the entire model grid. The top of the 1 m thick clay layer was located at a depth of 6 m (layer 7 of the model). The plume of simulation 1 was superimposed onto these new, baseline conditions in layers 1 through 6. The base of the plume was in direct contact with the buried clay layer. Figure 7 is a contour map of the difference dipole between  $E_0$  and  $E_s$  for these conditions. As this figure shows, except for a slight change in the magnitude of the contours, the difference dipole shape is very similar to the homogeneous and isotropic case (Figure 4).

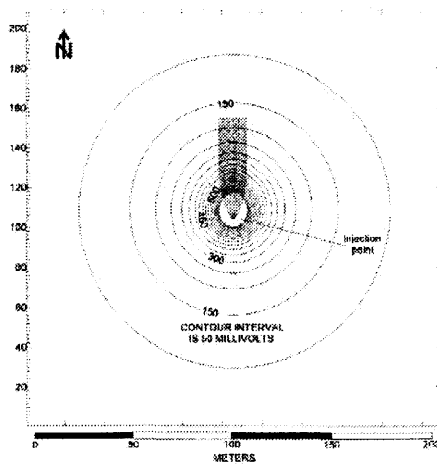


Figure 3. New electrical potential field with plume present in a homogenous and isotropic aquifer.

#### Simulation 4

Baseline conditions for simulation 4 consisted of an aquifer overlain by a conductive ( $\sigma_m=0.25$  S/m) clay layer. The 1 m thick clay layer extended over the entire model grid. The top of the clay was located at the land surface. The plume of simulation 1 was superimposed onto these baseline conditions immediately below the clay in layers 2 through 7. The current electrode was placed just below the clay in layer 2. The top of the plume (highest electrical conductivities) was in direct contact with the bottom of the clay. Therefore, the clay layer in effect became a uniform, electrically conductive extension of the plume. Figure 8 is a contour map of the difference dipole between  $E_0$  and  $E_s$  in layer 2 (at the top of the aquifer) for these conditions. Other than a change in magnitude and a slight change in the shape, the difference dipole was very similar to the contours for the buried clay layer (figure 7).

#### Simulation 5

Baseline conditions for simulation 5 consisted of an aquifer overlain by the same conductive ( $\sigma_m=0.25$  S/m) clay layer as in simulation 4. However, for this simulation, the top of the clay was located at the land surface and the current electrode was placed directly in the clay layer. Plume conditions were identical to those used in simulation 4.

- 37 -

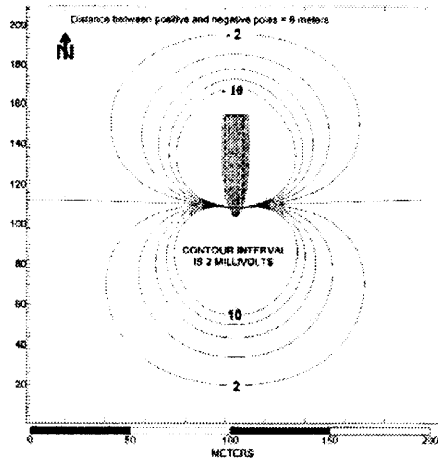


Figure 4. Numerical differences between the baseline electrical potential field and the electrical potential field with a plume present in a homogenous and isotropic aquifer.

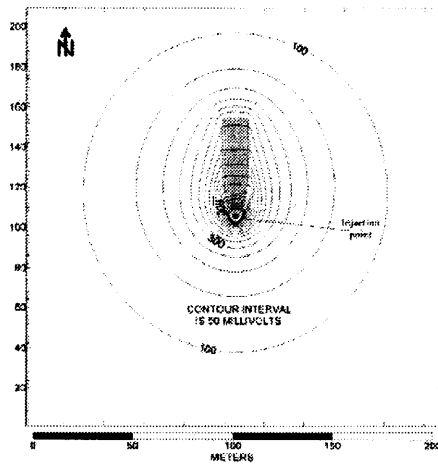


Figure 5. Electrical potential field for a plume-shaped clay pod in a homogenous and isotropic aquifer.

- 38 -

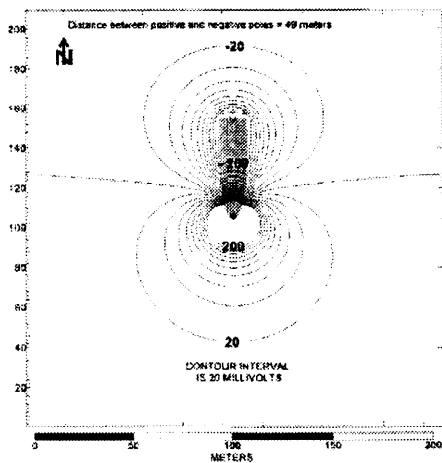


Figure 6. Difference dipole between the baseline electrical potential field with a plume-shaped clay pod present in a homogenous and isotropic aquifer.

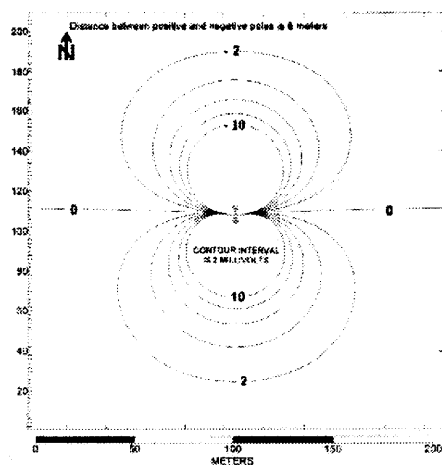


Figure 7. Difference dipole between the baseline electrical potential field with a bottom clay layer and the electrical potential field with a plume present above the clay.

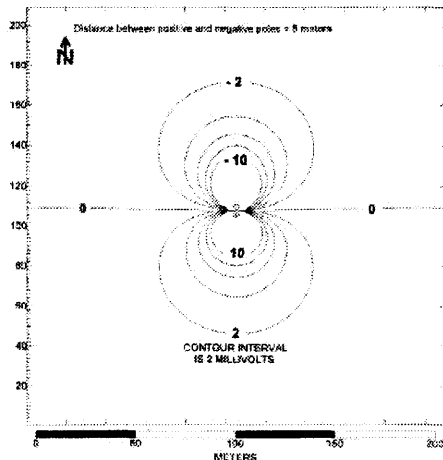


Figure 8. Difference dipole between the baseline electrical potential field with a clay top layer and the electrical potential field with a plume located beneath the clay. Electric current is injected into the plume below the clay layer in layer 2.

The top of the plume was in direct contact with the bottom of the clay and again the clay layer became an electrically conductive extension of the plume. This situation could occur during measurement of the electrical potential field, such as might be done to evaluate the integrity of a protective clay liner for a waste disposal pond or heap leach facility. Figure 9 is a contour map of the difference dipole between  $E_0$  and  $E_s$  measured in the clay layer if the current was injected into the clay instead of directly into the southernmost tip of the plume. Note that the generated difference dipole was smaller than for the other simulations and the negative side was significantly smaller than the positive side. Because the clay layer becomes an electrical extension of the plume, it is not surprising that the negative difference pole of the difference dipole does not delineate the center of mass of the actual plume. However, as figure 9 shows, the negative difference pole still occurs within 7 m of the known location of the plume center of mass.

#### Simulation 6

Baseline conditions consisted of an aquifer that contained a 100 m long, 10 m wide, north-south trending conductive ( $\sigma_m = 0.25$  S/m) buried clay lens. The top of the 1 m thick lens was located at a depth of 6 m. The rectangular lens extended 55 m north and 45 m south of the current electrode and 6 m west and 4 m east of the current electrode. The plume was superimposed onto baseline conditions in layers 1 through 6 for this simulation. The base of the plume (lowest electrical conductivities) was in direct contact with the top of the clay lens. Figure 10 is a contour map of the difference dipole between  $E_0$  and  $E_s$  for these conditions. These contours were very similar to the homogeneous and isotropic case except for a slight distortion in the negative contours near the southern end of the clay lens.

- 40 -

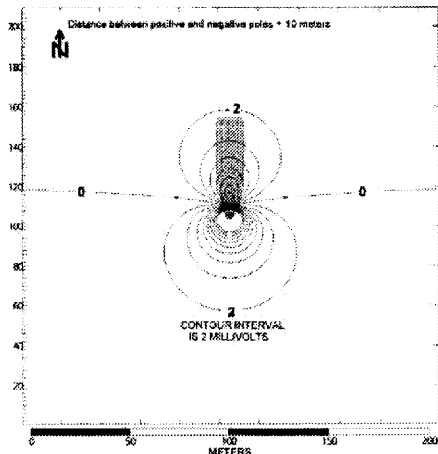


Figure 9. Difference dipole in layer 1 between the baseline electrical potential field with a clay top layer and the electrical potential field with a plume located beneath the clay. Electric current is injected into the clay layer (layer 1) immediately above the southernmost tip of the plume.

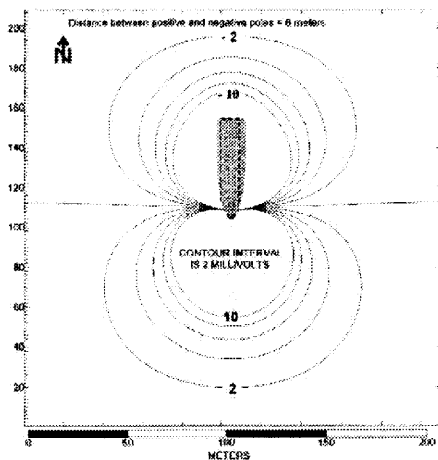


Figure 10. Difference dipole between the baseline electrical potential field with a buried, longitudinally-trending clay lens and the electrical potential field with a plume located above the lens.

- 41 -

#### Simulation 7

Baseline conditions consisted of an aquifer that contained a 100 m long, 10 m wide, east-west trending conductive ( $\sigma_m = 0.25$  S/m) buried clay lens. The top of the 1 m thick lens was located at a depth of 6 m. The rectangular lens extended 19 m to 29 m north of the current electrode and 50 m west and east of the current electrode. Lowest electrical conductivities at the base of the plume were in contact with the top of the clay lens. Figure 11 is a contour map of the difference dipole between  $E_0$  and  $E_s$  for these conditions. It is interesting that these contours were distinctly different from other simulations involving clay even though the lens was farther away. The primary reason for the unique distribution of electrical potential changes was the symmetrical geometry of intersection between the plume and the clay lens. The ends of the clay lens were clearly identifiable in the positive contours. The fact that the contours were positive at the ends of the clay lens illustrates that current flow was channeled into the lens under baseline conditions. However, with the plume present, a much more conductive pathway existed and electrical flow was now channeled preferentially past the lens to the end of the plume.

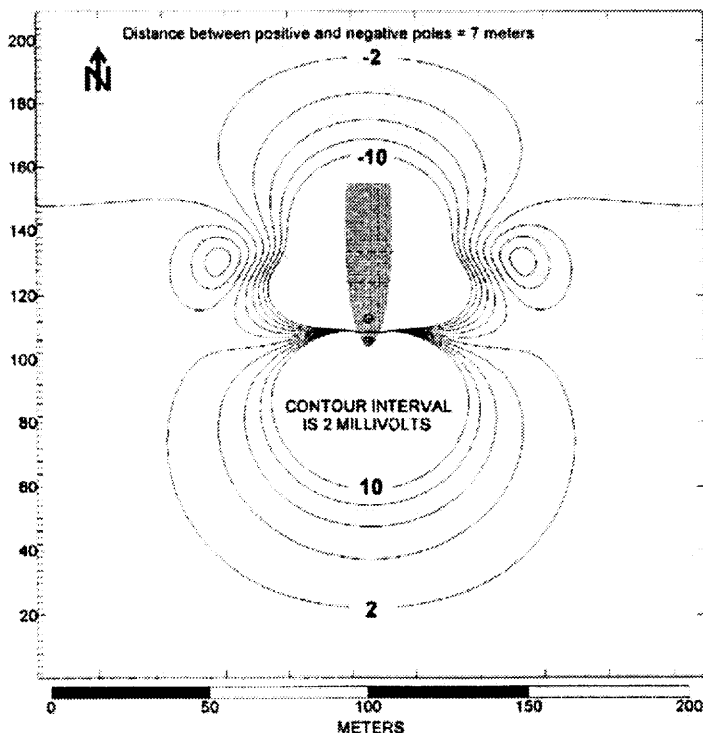


Figure 11. Difference dipole between the baseline electrical potential field with a buried transverse-trending clay lens and the electrical potential field with a plume located above the lens.

**SUMMARY**

The simulations illustrated the potential value of this approach, assuming continued technological advances in the field. The approximate location of the center of mass of a conductive contaminant plume and the direction of plume migration could be delineated by the mise-a-la-masse method. When a steady-state electric current was injected into the source of a contaminant plume, the resulting electrical potential field was distorted due to preferential channeling of current flow through the plume. Numerical differences between the baseline electrical potential field and a subsequent electrical potential field with a plume present formed a difference dipole. These distinct changes in the electrical potential distribution occurred even if layers or lenses of conductive clay were present. The distance between the positive and negative

- 43 -

difference poles represented the approximate distance to the center of mass of the plume from the plume source. In addition, a vector connecting the positive and negative difference poles pointed in the direction of plume migration.

#### REFERENCES

- Archie, G.E. 1942. The Electrical Resistivity Log as an Aid in Determining Some Reservoir Characteristics. Am. Inst. Min. Metallurg. Pet. Eng. Tech. Paper 1422, pp.146-154.
- Beasley C.W. and S.H. Ward, 1986. Three-dimensional Mise-a-la-masse Modeling Applied to Mapping Fracture Zones. *Geophysics*, v. 51, no. 1, pp. 98-113.
- Bevc, D. and H.F Morrison, 1989. Borehole-to-surface Electrical Resistivity Monitoring of a Salt Water Injection Experiment. Proceedings of the Society of Exploration Geophysicists 59<sup>th</sup> Annual International Exposition & Meeting, pp. 216-218.
- Bevc, D. and H.F Morrison, 1991. Borehole-to-surface Electrical Resistivity Monitoring of a Salt Water Injection Experiment. *GEOPHYSICS*, v. 56, no. 6, pp. 769-777.
- Bowker, A. 1987. Size Determination of Slab-like Ore Bodies - an Interpretation Scheme for Single Hole Mise-a-la-masse Anomalies. *Geoexploration*, v. 24, pp. 207-218.
- Dey, A. and H.F. Morrison, 1979. Resistivity Modeling for Arbitrarily Shaped Three-dimensional Structures. *Geophysics*, v. 44, no. 4, pp. 753-780.
- Domenico, P.A. and G.A. Robbins, 1985. A New Method of Contaminant Plume Analysis. *Ground Water*, v. 23, no. 4, pp. 486-485.
- Eloranta, E.H. 1985. A Comparison Between Mise-a-la-masse Anomalies Obtained by Pole-pole Electrode Configurations. *Geoexploration*, v. 23, pp. 471-481.
- Eloranta, E.H. 1986. The Behavior of Mise-a-la-masse Anomalies Near a Vertical Contact. *Geoexploration*, v. 24, pp. 1-14.
- Freeze, R.A., and J.A. Cherry, 1979. *Groundwater*. Prentice-Hall, Englewood Cliffs, NJ, 604pp.
- Jansen, J.R. and R.W. Taylor. 1995. Using MODFLOW to Model Several Geophysical Methods. Proceedings of the Symposium on the Application of Geophysics to Engineering and Environmental Problems, SAGEEP'95, Orlando, FL; EEGS, Englewood, CO, pp. 197-222.
- Keller, G.V. 1987. Rock and Mineral Properties. *Electromagnetic Methods in Applied Geophysics - Theory*, Volume 1, Society of Exploration Geophysicists, pp. 13-51.
- Ketola, M. 1972. Some Points of View Concerning Mise-a-la-masse Measurements. *Geoexploration*, v. 10, pp. 1-21.

- 44 -

Mansinha, L. and C.J. Mwenifumbo, 1983. A Mise-a-la-masse Study of the Cavendish Geophysical Test Site, *Geophysics*, v. 48, no. 9, pp. 1252-1257.

McClymont, G.L. and F.W. Schwartz, 1987. Development and Application of an Expert System in Contaminant Hydrogeology - The Expert ROKEY Computer System. Final Report and Users' Manual, Simco Groundwater Research Ltd., Alberta, Canada, 206 pp.

McDonald, M.G., and A.W. Harbaugh, 1988. A Modular Three-dimensional Finite-difference Ground-water Flow Model, Chapter A1, Book 6, *Techniques of Water-Resources Investigations of the U.S. Geol. Survey*.

Newkirk, D.J. 1982. Downhole Electrode Resistivity Interpretation with Three-dimensional Models: Dept. of Geology and Geophysics, University of Utah Technical Report DOE/ID/12079-47 for the U.S. Dept. of Energy.

Osiensky, J.L. 1995. Time Series Electrical Potential Field Measurements for Early Detection of Ground Water Contamination. *J. Environ. Sci. Health*, A30(7): 1601-1626.

Osiensky, J.L. and P.R. Donaldson, 1994. A Modified Mise-a-la-masse Method for Contaminant Plume Delineation. *Ground Water*, v. 32, no. 3, pp.448-457.

Osiensky, J.L. and P.R. Donaldson, 1995. Electrical Flow Through an Aquifer for Contaminant Source Leak Detection and Delineation of Plume Evolution. *Journal of Hydrology*, v. 169/1-4, pp. 243-263.

Osiensky, J.L. and R.E. Williams, 1996. A Two-dimensional MODFLOW Numerical Approximation of Mise-a-la-masse Electrical Flow Through Porous Media. *Ground Water*, v. 34, no. 4, pp.727-733.

Osiensky, J.L. 1997. Ground Water Modeling of Mise-a-la-masse Delineation of Contaminated Ground Water Plumes. *Journal of Hydrology*, 197(1997), pp.146-165.

Parasnis, D.S. 1967. Three-dimensional Electric Mise-a-la-masse Survey of an Irregular Lead-zinc-copper Deposit in Central Sweden. *Geophys. Prosp.*, v. 15, no. 3, pp.407-437.

Parasnis, D.S. 1997. *Principles of Applied Geophysics*. Chapman & Hall, London, 429 pp.

Parkhomenko, E.I. 1967. *Electrical Properties of Rocks*, Monographs in Geoscience, Plenum Press, New York, 314 pp.

Schlumberger, C. 1920. *Etude Sur la Prospection Electrique du Sous-sol*. Gauthier-Villars, Paris, 94 pp.

Wilt, M.J. and C.F. Tsang, 1985. Monitoring of Subsurface Contaminants with Borehole/surface Resistivity Measurements. Lawrence Berkeley Laboratory Report LBL-19106, pp 167-177.